The mathematical modelling of the motion of a horizontal vibrating screen supported by ROSTA oscillating mountings

J. A. Snyman* and P. J. Vermeulen*
University of the Pretoria
(First received August 1991, Final Form April 1992)

Summary

A versatile mathematical model of the behaviour of a vibrating conveyor screen supported by ROSTA oscillating mountings is developed. The model allows for various configurations through the specification of different screen and vibrating motor characteristics, connecting rod lengths, torsional stiffnesses of suspension units and mounting positions and orientations. The model is implemented in a computer program which allows for the computation of the time variation of the reactions and couples at the foundation supports and the horizontal, vertical and angular displacements of the screen. The validity of the model is verified by comparison of the predicted behaviour against the experimentally determined motion of a real vibrating screen. The model may be used to prescribe mounting configurations which, subject to design constraints, give minimum transmission of forces into the supporting structure.

Introduction

Vibratory conveyors are used to convey a wide variety of materials ranging from dry powders to heavy block castings. They offer many unique advantages such as conveying of materials at elevated temperatures, combining operations like cooling, drying, blending and screening with conveying [1-4]. In the modern vibratory conveyor the horizontal oscillating trough vibrates at small amplitudes and high frequency. Drives with double rotating imbalances produce a periodic force excitation, usualy at an angle of 45° to the vertical, such that the material being conveyed periodically loses contact with the trough. During this jump phase the material moves forward due to the horizontal momentum imparted to it by the trough before loss of contact. Fig. 1 gives a diagrammatic representation of such a conveying trough mounted on helical compression springs.

Of particular interest in this study are the trough supports. They play a decisive role in determining the stroke amplitude and the magnitude of the forces transmitted to the foundations. Traditionally helical steel springs, hollow or solid rubber springs and air cushion supports are used. Under certain operating conditions these traditional supports perform poorly. The helical springs and air cushions may, for example, collapse without warning resulting in maintenance problems. One of the main objections to the traditional supports in the case of vibratory conveyors is that they result in poor directional screen control, allowing the screen to float and oscillate laterally and perpendicular to the feed direction. As a result attention has lately shifted to the use of ROSTA suspension mountings.

A typical ROSTA mounting is depicted in Fig. 2. It consists of 3 rods (ℓ_1, ℓ_2 and ℓ_3) linked together by two supsension units housed in the central rod as shown. The

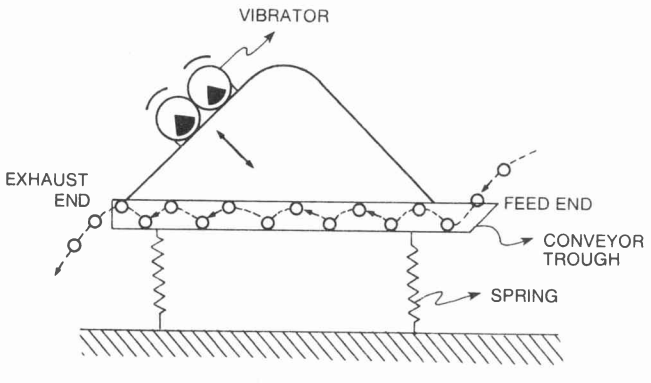

Figure 1 – Diagrammatic representation of conveying trough mounted on springs

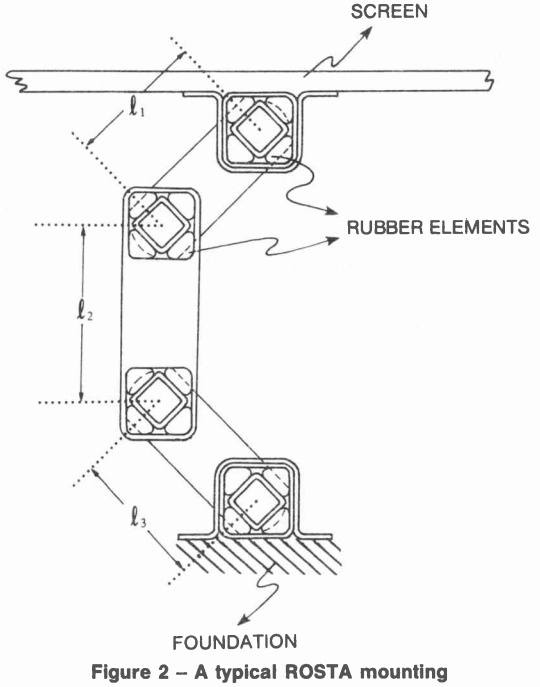

Figure 2 – A typical ROSTA mounting

* Professors
Centre for Structural Mechanics
Department of Mechanical Engineering
University of Pretoria
0002 Pretoria

top and bottom rod is attached to the screen and foundation through units respectively secured to the screen and foundation. The individual suspension units consist of four prestressed special rubber elements between an outer case and a square inner core canted at 45 degrees. The inner core can thus rotate through a torsion angle of up to $\pm$ 30° relative to the outer case [5]. The top and bottom rods are rigidly attached to the square inner cores allowing them to rotate relative to the central rod, the screen and the foundation. The mountings support the screen with the rods in the plane of motion, which results in excellent directional control.

For the ROSTA mountings the transmission of forces into the foundation is, however, highly dependent on a correct choice of the mounting characteristics, namely the lengths of the rods ℓ_1, ℓ_2 and ℓ_3 and the torsional stiffnesses of the individual suspension units. The stiffnesses and load capacity of the suspension units may be varied by adjusting the dimensions of the outer case and inner core as well as the total length of the suspension units. Accordingly the units are available in different models and sizes from the manufacturer [5].

In order to achieve a suitable design of the suspension mountings for a horizontal vibrating screen it is essential that a facility be available for the evaluation of the performance of various proposed configurations. In particular it is of interest to know how the transmissibility of forces into the supporting structure is affected by varying different design parameters such as, for example, the stiffnesses of the ROSTA suspension units, the lengths of the connecting rods between the units and the positioning and input of the eccentric vibrators. In addition, the detailed motion of any specified point on the screen as a function of the parameters may be of interest, in order to obtain optimal conveyor characteristics.

To do the required routine evaluation experimentally in the laboratory is clearly an expensive and cumbersome operation if one wishes to investigate a wide range of different possible configurations. An attractive alternative is to construct a reliable and general mathematical model of the screen-suspension system. Such a model, once computerised, will make it possible to compute with relative ease the behaviour of any specified system. This will allow comparisons to be made so that the design may be optimized. According to the representative [6] of the manufacturing company no such mathematical model exists as yet. Indeed it appears from a survey of the available literature that even for conveyors with traditional supports most of the published work is either of an empirical nature or the proposed mathematical models are oversimplified. Typical of the latter case is the work of Winkler [7] and of Ganapathy and Parameswaran [8].

The purpose of this study is therefore to develop a mathematical model of a fairly general screen-suspension system in which ROSTA-based suspension mountings are used. The validity of the model is proved by comparison of computer predictions against the experimentally measured performance of a real vibrating screen.

The model

The model to be analyzed here is depicted in Fig. 3(a). The screen is supported by four mountings (two in front and two behind), each consisting of four ROSTA suspension units, not necessarily identical, that are joined to each other by connecting levers as shown. The axes of the suspension units are perpendicular to the x-y plane thus restricting motion to the x-y plane. The mountings are of type AB (see ROSTA catalogue [5]) in which units 2 and 3 (see Fig. 3(a)) are rigidly joined by a lever of length ℓ_2. Similarly units 6 and 7 are also rigidly connected. Units 1 and 5 connect the screen to the mountings and the mountings are secured to the supporting foundation through units 4 and 8. In the unstrained position all the indicated angles (α, β, γ, ϕ, α', β', γ', ϕ') are equal to 45° except $\theta = 0°$. The corresponding torsion angles are therefore given by the specified angle minus 45° (see Fig. 3 (b)). The position of the centre of mass G relative to the indicated origin is (x_G, y_G) and the angle through which the screen rotates relative to the horizontal is denoted by θ. The position of G relative to the screen supports are specified by the distances a, b and h.

From the above it is clear that once the parameters (ℓ_1, ℓ_2, ℓ_3, a, b, h) are fixed then the orientation and position of the system is completely specified by the 11 coordinates (x_G, y_G, θ, α, β, γ, ϕ, α', β', γ', ϕ'). Indeed these coordinates overdetermine the system since relationships exist be-

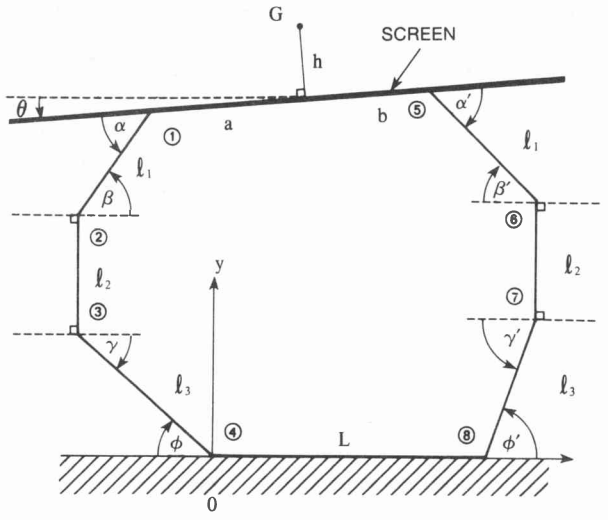

Figure 3(a) – Diagrammatic representation of the screen model to be analyzed

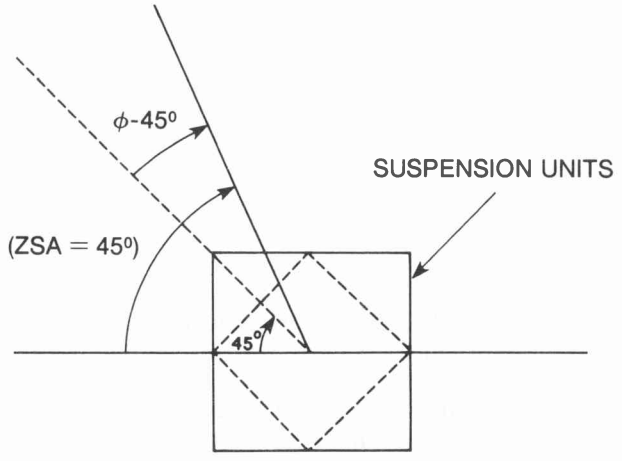

Figure 3(b) – Typical torsion angle

tween them, which means that they are not all independent. Appendix A shows that 6 such constraint relationships exist, leaving only 5 independent variables, i.e. the system may be precisely specified by a minimum of 5 coordinates and therefore has only 5 degrees of freedom. For convenience the 11 coordinates above are denoted by the respective components of the vector $\mathbf{q} = [q_1, q_2, \ldots, q_{11}]^T$. The six constraints, which are specified in detail in Appendix A, may then be briefly written as

$$g_j(\mathbf{q}) = 0, j = 1,2,\ldots,6 \tag{1}$$

Equations of motion

It is assumed that the masses of the connecting levers are negligible in comparison with the mass of the screen. Also, for the moment, assume no damping and no applied disturbing force, i.e. an undamped free system. Lagrange's equations of motion with constraints [9, 10] may now be applied to the system.

The expression for the kinetic energy of the system is

$$T = \tfrac{1}{2}m\dot{q}_1^2 + \tfrac{1}{2}m\dot{q}_2^2 + \tfrac{1}{2}I_G\dot{q}_3^2 \tag{2}$$

where m denotes the mass of the screen, I_G the mass moment of inertia of the screen about the z-axis through G and . denotes the time derivatives. The potential energy is given by

$$V = \sum_{i=4}^{11}\int_{\frac{\pi}{4}}^{qi} K_i[q_i - \frac{\pi}{4}]dq_i + mgy_G \tag{3}$$

where $K_i[q_i - \frac{\pi}{4}]$ denotes the torque exerted in Nm by the suspension unit corresponding to coordinate q_i at torsion angle $q_i - \frac{\pi}{4}$, which is measured in radians. The acceleration due to gravity is denoted by g.

For each coordinate q_i the Lagrange equation is applied in the following form:

$$\frac{d}{dt}(\frac{\partial L}{\partial \dot{q}_i}) - \frac{\partial L}{\partial q_i} = \sum_{j=1}^{6}\lambda_j h_{ji},\ i = 1,2,\ldots,11 \tag{4}$$

where $L = T - V$, $h_{ji} = \dfrac{\partial g_j}{\partial q_i}$ and the undetermined Lagrange multipliers, one corresponding to each constraint in (1), denoted by λ_j. In general these multipliers will also be time dependent.

Reverting back to the original notation for the coordinates, the application of (4) yields the following eleven important equations.

$$I_G\ddot{\theta} = \lambda_1(a+b)cos\theta - \lambda_2(a+b)sin\theta + \lambda_4 + \lambda_5(asin\theta + hcos\theta) - \lambda_6(a\cos\theta - hsin\theta) \tag{5.1}$$

$$m\ddot{x}_G = \lambda_5 \tag{5.2}$$

$$m\ddot{y}_G = \lambda_6 - mg \tag{5.3}$$

$$K_\alpha[\alpha - \frac{\pi}{4}] = -\lambda_3 + \lambda_4 \tag{5.4}$$

$$K_{\alpha'}[\alpha' - \frac{\pi}{4}] = -\lambda_3 \tag{5.5}$$

$$K_\beta[\beta - \frac{\pi}{4}] = \lambda_1\ell_1 cos(\gamma - \phi + \beta) - \lambda_2\ell_1 sin(\gamma - \phi + \beta) + \lambda_3 - \lambda_4 + \lambda_5\ell_1 sin(\gamma - \phi + \beta) - \lambda_6\ell_1 cos(\gamma - \phi + \beta) \tag{5.6}$$

$$K_{\beta'}[\beta' - \frac{\pi}{4}] = -\lambda_1\ell_1 cos(\gamma' - \phi' + \beta') - \lambda_2\ell_1 sin(\gamma' - \phi' + \beta') + \lambda_3 \tag{5.7}$$

$$K_\gamma[\gamma - \frac{\pi}{4}] = (\lambda_6 - \lambda_1)\{\ell_2 sin(\gamma - \phi) - \ell_1 cos(\gamma - \phi + \beta)\} + \lambda_3 - \lambda_4 + (\lambda_5 - \lambda_2)\{\ell_2 cos(\gamma - \phi) + \ell_1 sin(\gamma - \phi + \beta)\} \tag{5.8}$$

$$K_{\gamma'}[\gamma' - \frac{\pi}{4}] = (\lambda_1\{\ell_2 sin(\gamma' - \phi') - \ell_1 cos(\gamma' - \phi' + \beta')\} - \lambda_2\{\ell_2 cos(\gamma' - \phi') + \ell_1 sin(\gamma' - \phi' + \beta')\} + \lambda_3 \tag{5.9}$$

$$K_\phi[\phi - \frac{\pi}{4}] = (\lambda_1 - \lambda_6)\{\ell_3 cos\phi + \ell_2 sin(\gamma - \phi) - \ell_1 cos(\gamma - \phi + \beta)\} - \lambda_3 + \lambda_4 + (\lambda_2 - \lambda_5)\{\ell_3 sin\phi + \ell_2 cos(\gamma - \phi) + \ell_1 sin(\gamma - \phi + \beta)\} \tag{5.10}$$

$$K_{\phi'}[\phi' - \frac{\pi}{4}] = -\lambda_1\{\ell_3 cos\phi' + \ell_2 sin(\gamma' - \phi') - \ell_1 cos(\gamma' - \phi' + \beta')\} + \lambda_2\{\ell_3 sin\phi' + \ell_2 cos(\gamma' - \phi') + \ell_1 sin(\gamma' - \phi' + \beta')\} - \lambda_3 \tag{5.11}$$

Solution of equations of motion

The main objective is the solution of equations of motion (5.1) to (5.3) which will give the time dependent behaviour of x_G, y_G and θ. Their solution clearly requires the availability of the time dependent multipliers $\lambda_j, j = 1, 2, \ldots, 6$. The $\lambda_j's$ may be solved for in the following way: eq (5.5) gives λ_3, after which (5.4) yields λ_4; with λ_3 and λ_4 known one may simultaneously solve (5.7) and (5.9) for λ_1 and λ_2 and follow this up by the simultaneous solution of (5.6) and (5.8) to yield λ_5 and λ_6. Details of the solutions of the multipliers are given in Appendix B. Notice that the solution of the $\lambda_j's$ is in terms of the time dependent suspension unit angles $q_4, q_5, \ldots, q_{11}$. Eqs (5.1) to (5.3) therefore take on the general form:

$$\begin{aligned}\ddot{q}_1 &= f_1(q_1,q_2,\ldots,q_{11}) = f_1(\mathbf{q})\\ \ddot{q}_2 &= f_2(\mathbf{q})\\ \ddot{q}_3 &= f_3(\mathbf{q})\end{aligned} \tag{6}$$

To solve for all the $q_i's$ a further 8 *independent* differential equations in $\mathbf{q}$ are required. Keep in mind that in solving for the $\lambda_j's$ equations (5.10) and (5.11) were not used. If the

solutions for the $\lambda_j's$ are now substituted in (5.10) and (5.11) both relationships may be written in the form:

$$\ell_j(q_1,q_2,\ldots,q_{11}) = 0, j = 1,2 \tag{7}$$

By differentiating the above the following differential forms are obtained:

$$\sum_{i=1}^{11}\frac{\partial l_j}{\partial q_i}\dot{q}_i = 0, j = 1,2 \tag{8}$$

A further 6 differential equations are required. These may be obtained from the constraint equations (1) which are detailed in Appendix A. Again by differentiation the differential forms of the constraint equations are:

$$\sum_{i=1}^{11}\frac{\partial g_j}{\partial q_i}\dot{q}_i = 0, j = 1,2,\ldots,6 \tag{9}$$

Equations (8) and (9) may now be combined in the matrix equation:

$$\begin{bmatrix} \frac{\partial \ell_1}{\partial q_4} & \frac{\partial \ell_1}{\partial q_5} & \cdots & \frac{\partial \ell_1}{\partial q_{11}} \\ \frac{\partial \ell_2}{\partial q_4} & \frac{\partial \ell_2}{\partial q_5} & \cdots & \frac{\partial \ell_2}{\partial q_{11}} \\ \frac{\partial g_1}{\partial q_4} & & \cdots & \frac{\partial g_1}{\partial q_{11}} \\ \vdots & & & \vdots \\ \frac{\partial g_6}{\partial q_4} & & \cdots & \frac{\partial g_6}{\partial q_{11}} \end{bmatrix} \begin{bmatrix} \dot{q}_4 \\ \dot{q}_5 \\ \dot{q}_6 \\ \vdots \\ \dot{q}_{11} \end{bmatrix} = - \begin{bmatrix} \Sigma_{i=1}^{3} \frac{\partial \ell_1}{\partial q_i}\dot{q}_i \\ \Sigma_{i=1}^{3} \frac{\partial \ell_2}{\partial q_i}\dot{q}_i \\ \Sigma_{i=1}^{3} \frac{\partial g_1}{\partial q_i}\dot{q}_i \\ \vdots \\ \Sigma_{i=1}^{3} \frac{\partial g_6}{\partial q_i}\dot{q}_i \end{bmatrix}$$

which may be written more concisely as

$$\mathbf{A}\dot{\mathbf{q}}' = \mathbf{c} \tag{10}$$

or

$$\dot{\mathbf{q}}' = \mathbf{A}^{-1}\mathbf{c} \tag{11}$$

where $\mathbf{q}' = [q_4,q_5,\ldots,q_{11}]^T$.

Equations (6) and (11) form a system of 11 simultaneous differential equations which may now be solved to give $q_1,q_2,\ldots,q_{11}$ as functions of time.

Simultaneously with the solution of $\mathbf{q}(t)$ we may compute $\lambda(t) = [\lambda_1(t),\lambda_2(t),\ldots,\lambda_6(t)]^T$ by using the expressions for $\lambda(t)$ given in Appendix B.

It can be shown (see Appendix C and Fig. 4) that the relationships between the $\lambda_j's$ and the vertical and horizontal reactions at the screen supports (and the foundations) are given by

$$\begin{aligned} S_x &= \lambda_2,\ R_x = \lambda_5 - \lambda_2 \\ S_y &= \lambda_1,\ R_y = \lambda_6 - \lambda_1 \end{aligned} \tag{12}$$

This allows for the computation of the time variation of the reactions as the $\lambda_j(t)'s$ become available. At the same time the couples transmitted to the foundations may also be computed from the torque angles $\phi(t)$ and $\phi'(t)$ by

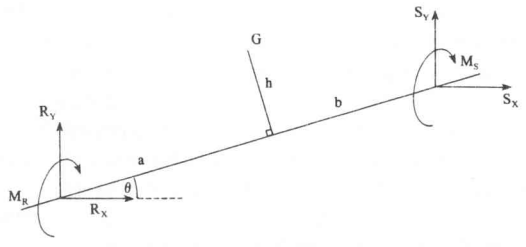

Figure 4 – Vertical and horizontal reactions at the screen supports

$$M_\phi(t) = K_\phi[\phi(t) - \frac{\pi}{4}] \text{ and } M_{\phi'}(t) = K_{\phi'}[\phi'(t) - \frac{\pi}{4}] \tag{13}$$

Inclusion of disturbing and damping forces

A periodic disturbing force may now be introduced via two eccentric synchronised motors. Allowing for an effective eccentric mass μ rotating at a radius r with angular frequency ω gives an amplitude (see Fig. 5)

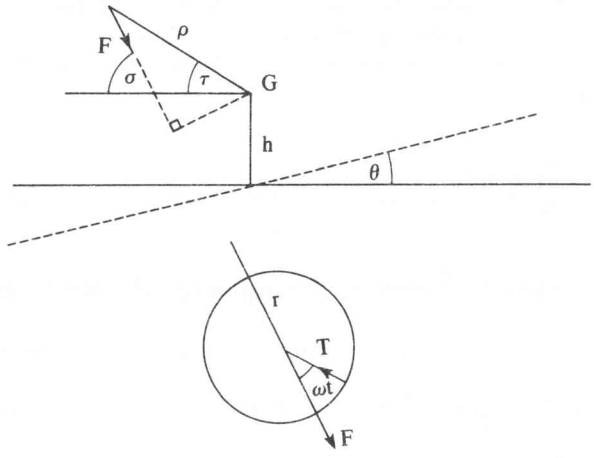

Figure 5 – The disturbing force F and its line of action relative to the centre of mass G

$$T = \mu r\omega^2 \tag{14}$$

The corresponding periodic disturbing force is

$$F = T\cos(\omega t) \tag{15}$$

acting at a vector position $\boldsymbol{\rho}$, specified by ρ and τ (see Fig. 5), from the centre of mass G and acting in the direction shown. In our model we allow for the possibility that the line of action of F may not be through G, making an angle $\sigma(\neq\tau)$ with the base of the screen. Allowing for the rotation θ of the screen the additional force components to be accommodated in (5.2) and (5.3) respectively are

$$\begin{aligned} F_x &= F\cos(\sigma - \theta) \\ F_y &= -F\sin(\sigma - \theta) \end{aligned} \tag{16}$$

The corresponding additional moment to be included in (5.1) is

$$M_\theta = F_\rho sin(\sigma - \tau) \quad (17)$$

Usually we have $\sigma = \tau = 45°$.

It is assumed that the damping moment and forces are proportional to the velocities and are of the form

$$\begin{aligned} T_\theta &= -C_\theta I_G \dot{\theta} \\ T_x &= -C_x m\dot{x} \\ T_y &= -C_y m\dot{y} \end{aligned} \quad (18)$$

The values of the damping constants may be determined experimentally. We obtain a complete description of the motion by including the respective damping terms above in the corresponding equations of motion (5.1), (5.2) and (5.3).

Computational experiments

For its verification and analysis the mathematical model was implemented in a CSMP computer program, and applied to an experimental set up consisting of a Vibramech 600 × 2400 vibrating screen [11] supported by a system of ROSTA type AB 38 × 80 mm oscillating mountings [5]. The screen is driven by two Uras vibrating motors, type KEE-13-6, running in opposite directions to each other at a frequency of 16 Hz so that they automatically synchronise to produce a straight line motion [12]. The motors are mounted such that the line of action of the vibrating force is through G at an angle of 45° with respect to the horizontal base of the screen (i.e. $\tau = \sigma = 45°$). The maximum force of each motor is 1 300 kg force. The total mass of the screen is taken as 700 kg and the mass moment of inertia of the screen, $I_G = 372\ kg\ m^2$. The values of the damping constants, determined experimentally by logarithmic decrement, are $C_\theta = 2{,}64s^{-1}$, $C_x = 1{,}61s^{-1}$ and $C_y = 2{,}39s^{-1}$ respectively.

At the exhaust end (position R in fig. 4) the screen is supported symmetrically, at the back and front by, in each case, two AB 38 × 80 ROSTA anti-vibration mountings and at the feed end (position S) by two mountings, one at the back and one in front. The double mountings on the left were modelled as single systems with the suspension units having double the torsional stiffnesses.

In the zero strain position the angle (ZSA) which the top (and bottom) rods of the mountings make with the horizontal, measured anti-clockwise downward, is equal to 45° (i.e. the specification of ZSA = 45° corresponds to the initial configuration $\alpha = \beta = \gamma = \phi = 45°$; $\alpha' = \beta' = \gamma' = \phi' = 135°$, and may be indicated by "position" [[-[.) Other relevant specifications are: a = 0,52 m, b = 1,16 m, h = 0,305 m and L = 1,68 m. The lengths of the connecting rods for the initial experimental set up were: $\ell_1 = 120$ mm, $\ell_2 = 60$ mm and $\ell_3 = 120$ mm.

Fig. 6 shows the computed (full circles) and experimentally determined variations of x_G and y_G with time. The computed stroke of 7,33 mm is in remarkable agreement with the experimentally observed stroke of 7,30 mm.

For the given experimental set up the computed variations (Δ's) in the horizontal and vertical reactions at the foundation supports are

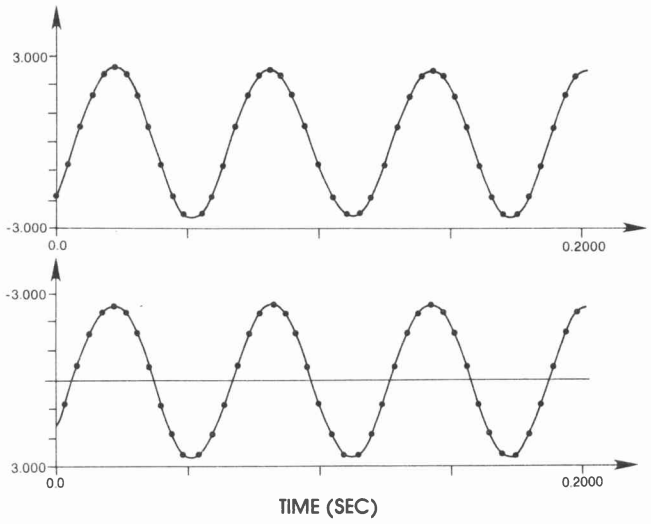

Figure 6 – Computed (full circles) and experimentally (line) determined variations of x_G and y_G with time

$$\Delta R_x = 116\ N \qquad \Delta S_x = 51\ N$$
$$\Delta R_y = 262\ N \qquad \Delta S_y = 135\ N$$

The variations in the transmitted couples at the foundations are small:

$$\Delta M_\phi = 0{,}3\ Nm \text{ and } \Delta M_{\phi'} = 0{,}1\ Nm.$$

Clearly the major objective should be to seek alternative configurations which give reduced variations in the reactions. With this in mind the following computational experiments were performed.

Firstly ℓ_2 was kept fixed at $\ell_2 = 60$ mm and the computations were done for increasing values of $\ell_1 = \ell_3$. The results, depicted in Fig. 7, clearly show that increasing $\ell_1 = \ell_3$ drastically reduces the vertical Δ's whilst the

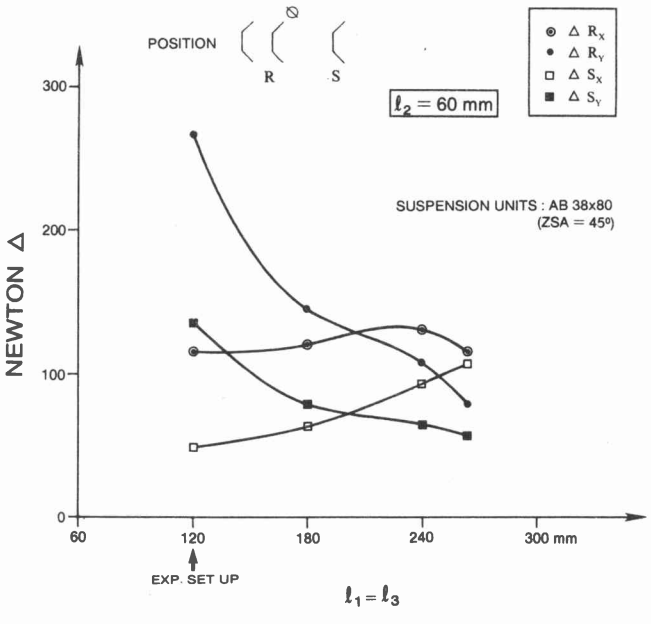

Figure 7 – Computed dependence of force variations (Δ's) on variation of $l_1 = l_3$ for fixed $l_2 = 60$ mm

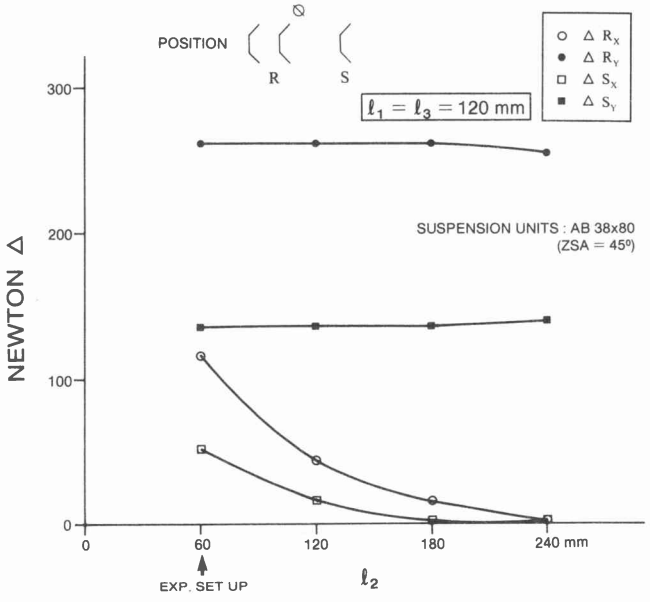

Figure 8 – Computed dependence of force variations (Δ's) on variation of l_2 for fixed values $l_1 = l_3 = 120$ mm

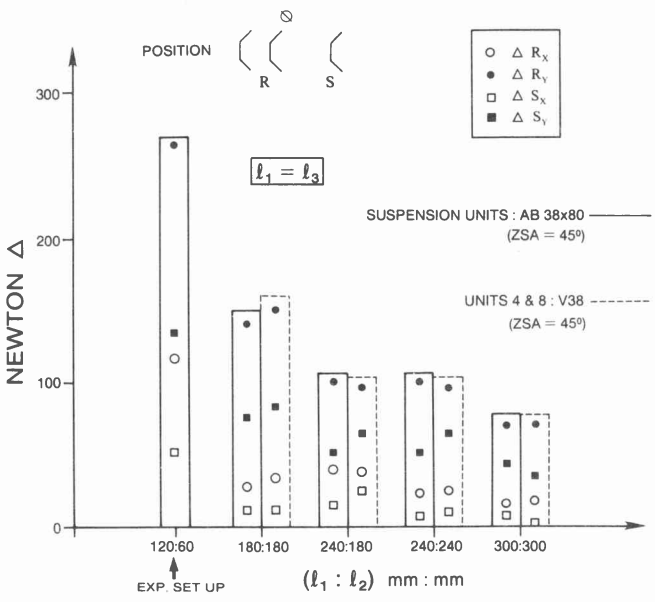

Figure 9 – Computed Δ's for a number of combinations of $l_1 : l_2$ with $l_1 = l_3$

horizontal Δ's remain effectively unchanged. Of course there is a limit to the allowable increase in ℓ_1 and ℓ_3 since the torsion angles should remain within the permissable range of $\pm 30°$, which is the case here even up to the value $\ell_1 = \ell_2 = 270$ mm. The variations in the transmitted couples, computed by equations (13), remain small with increasing $\ell_1 = \ell_3$ and therefore will not explicitly be referred to again in what follows. The stroke appears to be virtually unaffected by changes in ℓ_1 and ℓ_3 with a deviation of about 1% about the average value of 7,4 mm as the lengths were increased.

In the second experiment $\ell_1 = \ell_3$ was kept fixed at 120 mm and the Δ's were computed for increasing values of ℓ_2. Fig. 8 shows that in this case the horizontal Δ's decrease impressively whereas the vertical Δ's now remain virtually unchanged. Again the stroke remained effectively constant.

Figs 7 and 8 clearly suggest that for overall reduction in the Δ's, vertical and horizontal, both $\ell_1 = \ell_3$ and ℓ_2 should be increased. Consequently computations were done for a number of combinations of increased values of $\ell_1 : \ell_2$ (with $\ell_1 = \ell_3$). The results are indicated in Fig. 9 which shows that a considerable overall reduction (up to almost a factor of 4) may be obtained, compared to that of the experimental set up, if both ℓ_1 and ℓ_2 are increased. The above experiments were repeated with the foundation suspension units (i.e. units 4 and 8) replaced by stiffer units of the type V38 (for which the torque-angle characteristics were experimentally determined in the laboratory). The results are also shown in Fig. 9. No clear cut advantage seems to be obtained by using units V38 in place of the AB 38 × 80 units.

As a further demonstration of the versatility of the model the effect of alternative choices for the zero strain angle (ZSA) was investigated. Fig. 10 shows some results for the choices ZSA = 30° and ZSA = 60°. The results indicate that no appreciable gain is obtained with choices other than that of 45°. It is indeed important to note that the system does not appear to be very sensitive to changes in ZSA. Compare, for example, the results for

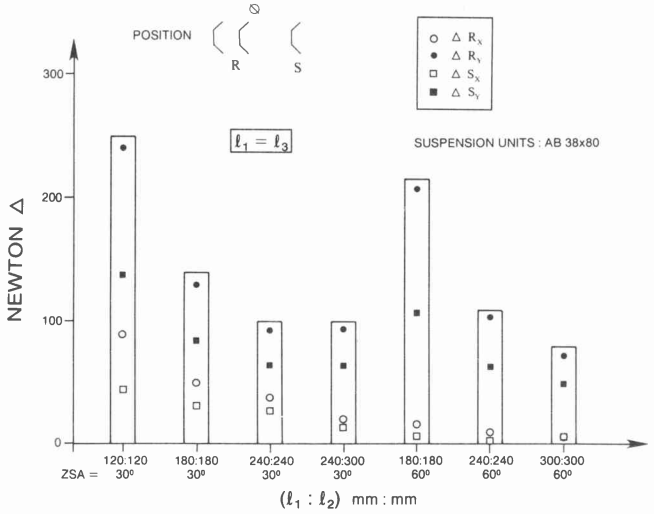

Figure 10 – Computed Δ's for alternative choices of zero strain angle (ZSA)

$\ell_1 : \ell_2 = 240 : 240$ in Figs. 9 and 10. These results seem to indicate that the system should not be too badly affected if appreciable sagging takes place.

So far the results are only for configurations in which the overall mounting position is of the form [[-[. Other possibilities corresponding to alternative positions such as [[-] and]]-] are also investigated. The results obtained for these alternative configurations were not significantly different.

The above experiments clearly indicate that significant reduction in the transmission of force variations may be obtained by lengthening the connecting rod lengths of the mountings. To ensure longevity of the units this should be done within the constraint that the torsion angles should *not exceed a maximum of 22°* throughout the motion [6].

To allow for a definite recommendation to be made with regard to the choice of lengths and suspension units for the specific Vibramech screen under consideration, the following final computational experiment was performed. For varying choices of the connecting rod

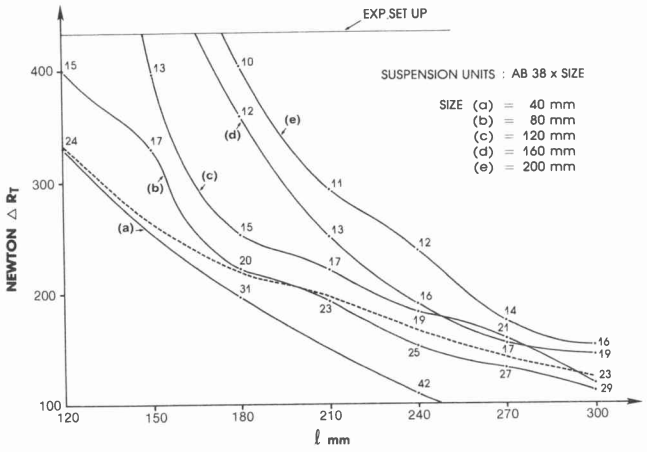

Figure 11 – Computed total resultant variation ΔR_T *as a function of* $l = l_1 = l_2 = l_3$ for different AB 38 suspension unit sizes

lengths, $\ell_1 = \ell_2 = \ell_3 = \ell$, the computations were performed for different AB38 unit sizes, namely 40; 80; 120; 160 and 200 mm. In each case the total resultant variation ΔR_T per side was calculated by

$$\Delta R_T = \{(\Delta R_x + \Delta S_x)^2 + (\Delta R_y + \Delta S_y)^2\}^{\frac{1}{2}}$$

and the torsion angles were monitored. The graph in Fig. 11 summarise the results. The indicated values on the graphs are the maximum torsion angle reached during vibration with the dashed line separating the acceptable configurations from those that exceed the set limit of 22°.

Quite clearly the "optimal" configurations are those in the bottom right hand corner, just above the dashed line.

On the basis of maximum reduction in force variation as well as acceptable maximum torsion angle a good configuration would be:

$$\ell_1 = \ell_2 = \ell_3 = 270 \text{ mm with units AB 38} \times 160$$

For this choice $\Delta R_T = 152{,}6$ N giving an overall reduction by a factor of 2,83. The computed stroke is 7,25 mm and the maximum torsion angle is 17,1° with a maximum amplitude of 1,0°. The individual Δ components are:

$\Delta R_x = 28{,}4N$ $\quad$ $\Delta S_x = 13{,}0N$
$\Delta R_y = 81{,}5N$ $\quad$ $\Delta S_y = 65{,}4N$

Should economy be an important factor, the use of smaller size units leads to the recommendation:

$$\ell_1 = \ell_2 = \ell_3 = 240 \text{ mm with units AB 38} \times 120$$

For this choice $\Delta R_T = 183{,}8$ N giving an overall reduction factor of 2,35. The computed stroke is 7,26 mm and the maximum torsion angle is 19,1° with a maximum amplitude of 1,2°. The individual Δ components are:

$\Delta R_x = 30{,}7N$ $\quad$ $\Delta S_x = 10{,}2N$
$\Delta R_y = 118{,}5N$ $\quad$ $\Delta S_y = 60{,}6N$

Conclusion

The overall objectives of this study have been accomplished. A versatile mathematical model of a vibrating screen supported by ROSTA oscillating mountings has successfully been developed. The model allows for various configurations through the specification of, amongst others, different screen and vibrating motor characteristics, connecting rod lengths, torsion stiffnesses of suspension units, and mounting positions and orientations. In particular the model enables the computation of the time variation of the reactions and couples at the foundation supports, the vertical and horizontal displacements as well as the angular rotation of the screen, and the variation with time of the torsion angles at all the suspension units.

The validity of the model was demonstrated by comparison of the predicted performance against the experimentally determined behaviour of a Vibramech vibrating screen. Sensitivity analysis by means of the model indicates that considerable reduction in the transmissibility of forces into the supporting foundation may be obtained by suitable changes in the configurational parameters of the system. In particular, lengthening of the connecting rods between suspension units results in significant reductions.

Finally, this study indicates that the mathematical model may successfully be applied to the analyses of many other systems currently in operation in industry.

Acknowledgements

The authors wish to thank Prof P S Heyns, Director of the Centre for Structural Mechanics for his encouragement and for initiating this project. Thanks also to Mr Hennie van Niekerk for experimental assistance and Mr Philip Maré of Oscillating Systems for his interest and permission to publish the findings of this study.

References

1. Paz, M., and Morris, J. M., "The Use of Vibration for Material Handling", *Journal of Engineering for Industry*, Transactions of the ASME, Series B, Vol.96, No.3, 1974, pp 735-740.
2. Parameswaran, M. A., and Ganapathy, S., "Vibratory Conveying – Analysis and Design: A Review", *Mechanism and Machine Theory*, Vol.14, 1979, pp 89-97.
3. Dumbaught, G. D., "The Evolution of the First Universal Vibratory Drive System for Moving and Processing Bulk Solid Materials", *Bulk solids handling*, Vol.4, No.1, 1984, pp 125-140.
4. Cuiying, Li, "Handling of Bulk Solids by Vibrating Machines", *Bulk solids handling*, Vol.6, No.6, 1986, pp 1147-1150.
5. ROSTA catalogue, ROSTA-WERK AG, CH-5502 Hunzenschwil, Switzerland.
6. Maré, P., Oscillating Systems (Pty) Ltd., Pretoria, Personal communication.
7. Winkler, G., "Analysing the Vibratory Conveyor", *Int. J. Mech. Sci.*, Vol. 20, 1978, pp. 561-570.
8. Ganapathy, S., and Parameswaran, M. A., "On the Design of the Unbalanced Mass Excited Vibratory Conveyor", *Bulk solids handling*, Vol.6, No.1, 1986, pp 59-63.
9. Fowles, G. R., "Analytical Mechanics", Holt Rinehardt and Winston, 1977.
10. D'Souza, A. F., and Garg, V. K., "Advanced Dynamics: Modelling and Analysis", Prentice-Hall Inc., 1984.
11. Vibramech brochure, Vibratory Equipment Specialists, P.O. Box 4189, Krugersdorp, Johannesburg.
12. Instruction manual for URAS vibrator, Murakami Seiki Manufacturing Co. Ltd., Kitakyushu, Japan.

Appendix A

Constraint equations

With reference to Fig. 3(a) and the 11 chosen coordinates, six constraint equations may be identified. Choosing the origin as indicated at the position of attachment of the left mounting to the foundation, the specification that the right mounting be secured at the position $(L, 0)$ yields the following two constraint equations.

$$g_1 = \ell_3 sin\phi + \ell_2 cos(\gamma - \phi) + \ell_1 sin(\gamma - \phi + \beta) + (a + b)sin\theta - \ell_3 sin\phi' - \ell_2 cos(\gamma' - \phi') - \ell_1 sin(\gamma' - \phi' + \beta') = 0 \quad (A.1)$$

and

$$g_2 = -\ell_3 cos\phi - \ell_2 sin(\gamma - \phi) + \ell_1 cos(\gamma - \phi + \beta) + (a + b)cos\theta - \ell_3 cos\phi' - \ell_2 sin(\gamma' - \phi') + \ell_1 cos(\gamma' - \phi' + \beta') - L = 0 \quad (A.2)$$

The third constraint follows from the geometric fact that the sum of the internal angles of the octagon defined by the screen, mountings and foundation floor (see Fig. 1(a)) is equal to 6π radians. Mathematically this reduces to

$$g_3 = \gamma + \gamma' + \beta + \beta' - \phi - \phi' - \alpha - \alpha' = 0 \quad (A.3)$$

The fourth constraint gives the relationship between the angle θ and the respective suspension unit angles:

$$g_4 = \theta - \gamma + \phi - \beta + \alpha = 0 \quad (A.4)$$

The final two constraints are derived from the expressions for the coordinates of the centre of mass G, (x_G, y_G), in terms of the suspension angles and the parameters of the system:

$$g_5 = x_G + \ell_3 cos\phi + \ell_2 sin(\gamma - \phi) - \ell_1 cos(\gamma - \phi + \beta) - acos\theta + hsin\theta = 0 \quad (A.5)$$

and

$$g_6 = y_G - \ell_3 sin\phi - \ell_2 cos(\gamma - \phi) - \ell_1 sin(\gamma - \phi + \beta) - asin\theta - hcos\theta = 0 \quad (A.6)$$

Appendix B

Solution of multipliers

From (5.5):

$$\lambda_3 = -K_{\alpha'}[\alpha' - \frac{\pi}{4}] \quad (B.1)$$

and from (5.4):

$$\lambda_4 = K_{\alpha}[\alpha - \frac{\pi}{4}] + \lambda_3 \quad (B.2)$$

Set

$$C' = \ell_1 cos(\gamma' - \phi' + \beta'),\ S' = \ell_1 sin(\gamma' - \phi' + \beta')$$
$$A' = \ell_2 sin(\gamma' - \phi') - \ell_1 cos(\gamma' - \phi' + \beta')$$
$$B' = \ell_2 cos(\gamma' - \phi') + \ell_1 sin(\gamma' - \phi' + \beta') \quad (B.3)$$

Solving (5.7) and (5.9) simultaneously for λ_2 and λ_1 gives:

$$\lambda_2 = \frac{A'\left\{\lambda_3 - K_{\beta'}\left[\beta' - \frac{\pi}{4}\right]\right\} + C'\left\{\lambda_3 - K_{\gamma'}\left[\gamma' - \frac{\pi}{4}\right]\right\}}{A'S' + B'C'} \quad (B.4)$$

and

$$\lambda_1 = \{\lambda_3 - \lambda_2 S' - K_{\beta'}[\beta' - \frac{\pi}{4}]\}/C' \quad (B.5)$$

Set

$$C = \ell_1 cos(\gamma - \phi + \beta),\ S = \ell_1 sin(\gamma - \phi + \beta)$$
$$A = \ell_2 sin(\gamma - \phi) - \ell_1 cos(\gamma - \phi + \beta)$$
$$B = \ell_2 cos(\gamma - \phi) + \ell_1 sin((\gamma - \phi + \beta) \quad (B.6)$$

Solving (5.6) and (5.8) simultaneously for λ_6 and λ_5 yields:

$$\lambda_6 = \{\lambda_1(SA + BC) + \lambda_3(B - S) + \lambda_4(S - B) + SK_{\gamma}[\gamma - \frac{\pi}{4}] - BK_{\beta}[\beta - \frac{\pi}{4}]\}/(AS + BC) \quad (B.7)$$

and

$$\lambda_5 = \{K_{\beta}[\beta - \frac{\pi}{4}] - \lambda_1 C + \lambda_2 S - \lambda_3 + \lambda_4 + \lambda_6 C\}/S \quad (B.8)$$

Appendix C

Solution of the reactions at the supports

With reference to Fig. 4 the classic equations of translational motion of the screen are given by:

$$m\ddot{x}_G = R_x + S_x \quad (C.1)$$

$$m\ddot{y}_G = R_y + S_y - mg \quad (C.2)$$

Clearly (C.1) corresponds to Lagrange equation (5.2) and (C.2) to (5.3) from which it follows that

$$R_x + S_x = \lambda_5 \quad (C.3)$$

$$R_y + S_y = \lambda_6 \quad (C.4)$$

The classic equation for the rotational motion of the screen is given by

$$I_G\ddot{\theta} = R_x(asin\theta + hcos\theta) + S_x(hcos\theta - bsin\theta) + S_y(hsin\theta + bcos\theta) - R_y(acos\theta - hsin\theta) + M_R + M_S \quad (C.5)$$

Utilising (C.3) and (C.4) reduces (C.5) to

$$I_G\ddot{\theta} = (R_x a - S_x b + \lambda_6 h)sin\theta + (\lambda_5 h + S_y b - R_y a)cos\theta + M_R + M_S \quad (C.6)$$

which corresponds to the Lagrange equation (5.1):

$$I_G\ddot{\theta} = (-\lambda_2(a + b) + \lambda_5 a + \lambda_6 h)sin\theta + (\lambda_1(a + b) + \lambda_5 h - \lambda_6 a)cos\theta + \lambda_4 \quad (C.7)$$

Comparing (C.6) with (C.7) gives

$$R_x a - S_x b = -\lambda_2(a + b) + \lambda_5 a \quad (C.8)$$

$$S_y b - R_y a = \lambda_1(a + b) - \lambda_6 a \quad (C.9)$$

From equation (C.3), (C.4), (C.8) and (C.9) R_x, R_y, S_x *and* S_y may be solved for to yield:

$$\begin{aligned} S_x &= \lambda_2,\ R_x = \lambda_5 - \lambda_2 \\ S &= \lambda_1,\ R = \lambda_6 - \lambda_1 \end{aligned} \quad (C.10)$$